Three-Dimensional Calculation of the Distribution of Eddy Currents and the Heating Effect on Slit Tubes when Welding Longitudinal Seams

R. Jürgens
AEG Elotherm
42855 Remscheid, Germany

U. Lüdtke and D. Schulze
Subdepartment of Electroheat, Technical University of Ilmenau
98684 Ilmenau, Germany

Abstract - **A numerical model is presented for the process of the inductive longitudinal-seal welding of tubes. This model refers to a three-dimensional, quasi-stationary electromagnetic field and a three-dimensional temperature field. The characteristics of the material dependent on the field in both cases are taken into consideration in iterative ways in the form of local functions. The differential equations describing the electromagnetic field are integrated as an A-φ formulation into the method of finite elements. The discretization, adapted to suit the problem, leads to grid networks with up to 100.000 nodes. The results of the calculations shown permit the determination of optimum process parameters.**

I. INTRODUCTION

The inductive longitudinal-seal welding of tubes is a technology for the manufacture of tubes that has been developed over the decades to achieve the present state of the art in production techniques.

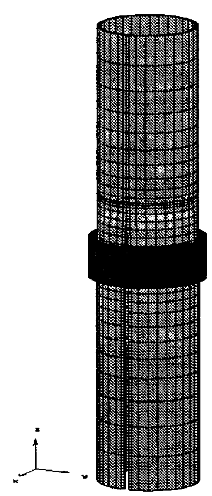

Fig. 1. Representation of the principle.

Tubes of all types of materials (e.g. Cu, brass, Al, Fe) and geometry (e.g. dia. 9 x 0,5 mm or dia. 508 x 16 mm) are produced according to this process. During the initial period of the technical development work was carried out employing mains frequency and medium frequency. High frequency, produced by valve generators, has been a decisive factor in the fabrication process for years.

This has not only had an effect upon the development of the hardware (some impeder materials are only suitable for the frequency range between 200 and 500 kHz), but also upon the development of the software. In this way, for example, with the BEM, a surface current covering the object and equivalent to the current is expected. This requires the skin effect to be complete.

In recent years, transistorised generators have become available operating at frequencies between 50 and 300 kHz. These generators are being employed with great success in the inductive welding of longitudinal tubes. The improvement in the quality of the welding seam is, in some cases, exception when compared with the welding seam produced using higher frequencies. In this case, the skin effect does not form completely.

In order to gain a deeper understanding of the welding process, a knowledge of the exact course of the temperature at the edges of the strip through the welding point and until the cooling-off, including all transformation processes, is essential. This does not only applies to the actual welding zone, but also to the adjacent zones, in which alterations in the structure are caused by the influence of the temperature.

A method of calculation is to be presented in the following, which from its nature is able to fulfil all these requirements.

II. MATHEMATICAL MODEL

Maxwell's equations form the basis for the calculation of the electromagnetic field

$$\mathrm{rot}\,\underline{\vec{H}} = \underline{\vec{J}} + \mathrm{j}\omega\underline{\vec{D}} \tag{1}$$

$$\mathrm{rot}\,\underline{\vec{E}} = -\,\mathrm{j}\omega\underline{\vec{B}} \tag{2}$$

together with the so-called material equations

$$\underline{\vec{J}} = \kappa\underline{\vec{E}} \tag{3}$$

$$\underline{\vec{B}} = \mu\underline{\vec{H}}. \tag{4}$$

Operating under the assumption that all magnetic quantities are sinusoidal with time, we work in complex domain. $\underline{\vec{D}}$, the

Manuscript received November 1, 1993.

0018-9464/94$4.00

change with time of the density of the displacement flow, is neglected. The density of the magnetic flux is freesource

$$\mathrm{div}\,\underline{\vec{B}} = 0 \tag{5}$$

and the magnetic vector potential $\underline{\vec{A}}$ as a mathematical subsidiary quantity

$$\underline{\vec{B}} = \mathrm{rot}\,\underline{\vec{A}}. \tag{6}$$

The magnetic vector potential is composed of a rotational field and a gradient field

$$\underline{\vec{A}} = \underline{\vec{A}}_w + \underline{\vec{A}}_\phi \tag{7}$$

with

$$\underline{\vec{A}}_\phi = \mathrm{grad}\,\underline{\phi}_A. \tag{8}$$

From the law of induction (2) and the definitions (6), (7), and (8), it follows that

$$\mathrm{rot}\,\underline{\vec{E}} = -j\omega\,\mathrm{rot}\left(\underline{\vec{A}}_w + \mathrm{grad}\,\underline{\phi}_A\right). \tag{9}$$

The integral counter-operation for the formation of rotation is applied to equation (9) to obtain

$$\underline{\vec{E}} = -j\omega\left(\underline{\vec{A}}_w + \mathrm{grad}\,\underline{\phi}_A\right) + \underline{\vec{E}}_0 \tag{10}$$

with

$$\underline{\vec{E}}_0 = -\mathrm{grad}\,\underline{\phi}_0. \tag{11}$$

The gradient field $\underline{\vec{E}}_0$ is produced as a quasi-integration constant, as

$$\mathrm{rot\ grad}\,\underline{\phi}_0 = 0. \tag{12}$$

a basic fact applies.
The impressed field strength $\underline{\vec{E}}_0$ is assumed to be source-free, so that the electrical potential $\underline{\vec{E}}_0$ is determined as follows

$$\mathrm{div\ grad}\,\underline{\phi}_0 = 0. \tag{13}$$

Behind the electric potential $\underline{\phi}_0$, there is the impressed inductor voltage. This assumption was confirmed by the calculation of the integral parameters of two- and three-dimensional arrangements. Derived from material equation (3) and formula (10), the important relationship for the calculation of the distribution of current density in the electrically-conductive regions results:

$$\underline{\vec{J}} = -j\omega\kappa\left(\underline{\vec{A}}_w + \mathrm{grad}\,\underline{\phi}_A\right) + \kappa\underline{\vec{E}}_0. \tag{14}$$

With the help of material equation (4), definition (6), and the relationship for the current density (14), the following differential equation results from the Maxwell's law (1):

$$\mathrm{rot}\frac{1}{\mu}\mathrm{rot}\,\underline{\vec{A}}_w + j\omega\kappa\left(\underline{\vec{A}}_w + \mathrm{grad}\,\underline{\phi}_A\right) = \kappa\underline{\vec{E}}_0. \tag{15}$$

Since in addition to $\underline{\vec{A}}_w$, $\underline{\phi}_A$ is also to be determined, the

$$\mathrm{div}\,\underline{\vec{J}} = 0 \tag{16}$$

is also explicitly required in equation (14), while taking relationship (13) into account:

$$\mathrm{div\,grad}\,\underline{\phi}_A + \mathrm{div}\,\underline{\vec{A}}_w = 0. \tag{17}$$

Together, equations (15) and (17) form the basis for the calculation of the electromagnetic field distribution and are also known as the A-ϕ formulation.

Special importance is assigned to the interface between conductive and non-conductive regions. The normal component of the resulting vector potential $\underline{\vec{A}}$ on the side of the electrically-conductive region must be zero, since according to equation (14), it determines the direction of the current density, and the current must not "flow out" from the conductive regions. In the electrically non-conductive regions, the scalar potential $\underline{\phi}_A$ is practically without any importance, that is, it may be assumed to be constant, since in the decisive equations, (14) and (15), it always occurs in connection with the electrical conductivity κ.

The heat-source density

$$p_v = \frac{|\underline{\vec{J}}|^2}{\kappa} \tag{18}$$

is calculated from the density of current distribution. The calculation of the temperature fields is effected on the basis of Fourier's heat-conduction equation [1]

$$\frac{\partial(c\rho\vartheta)}{\partial t} = \mathrm{div}(\lambda\,\mathrm{grad}\,\vartheta) + p_v - \vec{v}\,\mathrm{grad}(c\rho\vartheta) \tag{19}$$

with the velocity-vector field $\vec{v}$ taking into consideration the continuous feed process.

III. Numerical Model

The approximate calculation of the electromagnetic field is possible by the finite-element method using the Galerkin procedure on the differential equations (15) and (17). The necessary boundary, symmetrical and interface conditions are taken into account. An exhaustive description of the proce-

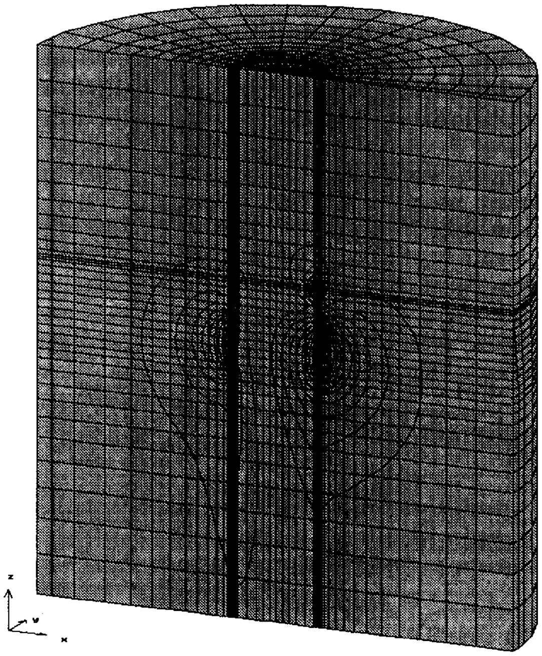

Fig. 2. Discretization of the computation zone and magnetic vector potential in the plane of symmetry.

dure for the A formulation (without scalar potential) is contained in [2], and for the A-ϕ formulation it is contained in [3] and [4].

The finite-element method requires the discretization of the bounded three-dimensional solution domain into volume elements. At the nodes thus produced, the discrete values of the vector potential $\underline{\vec{A}}_{w}$ and in the electrically-conductive zones, additionally the scalar potential $\underline{\phi}_{k}$ are sought as an unknown field quantity. The problem of the three-dimensional magnetic field is thus reduced to the solution of a system of linear algebraic equations. The matrix is positive definite, symmetrical, and sparsely occupied. A discretization adapted to the specific problem leads to grid networks containing up to 100,000 nodes or elements. A large matrix is produced, requiring storage forms that need little storage space. For the solution of the system of equations, the method of conjugated gradients is used as an iterative process to reach the solution [2].

The calculation of the temperature field is also carried out with the help of the finite element method (Galerkin procedure) on the basis of differential equation (19) [1]. Only the grid network of the tube is required. At the outer surface area, heat losses due to convection and radiation are taken into consideration. The calculation of the temperature field of the moving tube is performed with a fixed grid network. The feed is taken into account by the velocity vector $\vec{v}$, which results in an asymmetrical coefficient matrix. A biconjugated gradient process or a relaxation process is employed in the solution of the problem of the asymmetrical matrices. Since this is a real scalar field in this case, and the computation zone is restricted to the tube, resources for the solution of the system of equations are comparatively low.

In spite of the feed movement, a stationary temperature field is produced on the fixed grid network, and for this reason, the temperature field with feed movement may be regarded as a stationary-field problem. Trial calculations have, however, shown that with increasing feed velocity convergency problems with the iterative solution process begin and thus transient temperature field may be calculated. The feed velocities required, up to 1 m/s, could not be realised using this process. A way out of this problem is offered by the transient temperature-field calculation, where the Cranck-Nickelson process is employed [1]. Problems of convergency at increasing feed velocities may be countered by selecting shorter time intervals.

On the grid network of the tube (see Figure 1), the feed movement causes a entrance of mass on the side at which the tube enters, and a lost of mass on the tube's exit side. On the side at which the tube enters , the tube infeed temperature is determined from the first-kind boundary conditions. If these boundary conditions do not exist, instabilities will occur at high feed velocities. Individual nodes at the inlet side of the tube will be incorrectly heated to a high temperature. At the tube exit side, no negative effects of the mass exit were discovered.

For the discretization of the area for which the solutions is sought, a semi-automatic process using macro-elements is used [2]. Macro-elements are hexahedral, prisms and tetrahedral that are automatically meshed and then put together for the total discretization. The manual work required is limited to the definition of the macro-elements. Grid networks with 100,000 elements can, using this process, be constructed without any problem. The macro-element concept does not exclude input faults 100%, and for this reason, the completed discretization is tested for the meshing faults using a special program.

IV. Results

Figure 2 shows the finite element mesh used for calculating the electromagnetic field (16870 nodes, 15825 element's). Due to the symmetry of the arrangement, only one half of the computation area is meshed. The calculation is carried out on an efficient HP work station with 64 MB main memory.

Figure 2 shows a representation of the magnetic vector potential in the plane of symmetry. The areas of high current density are surrounded by the lines of isovector potential. Here, the inductor and the welding point on the tube may be clearly made out.

In Figure 3, the distribution of the current density on the surface of the tube is shown. It may be recognised that a great part of the eddy current flows over the welding point, but also a smaller one flows downward as "current leakage".

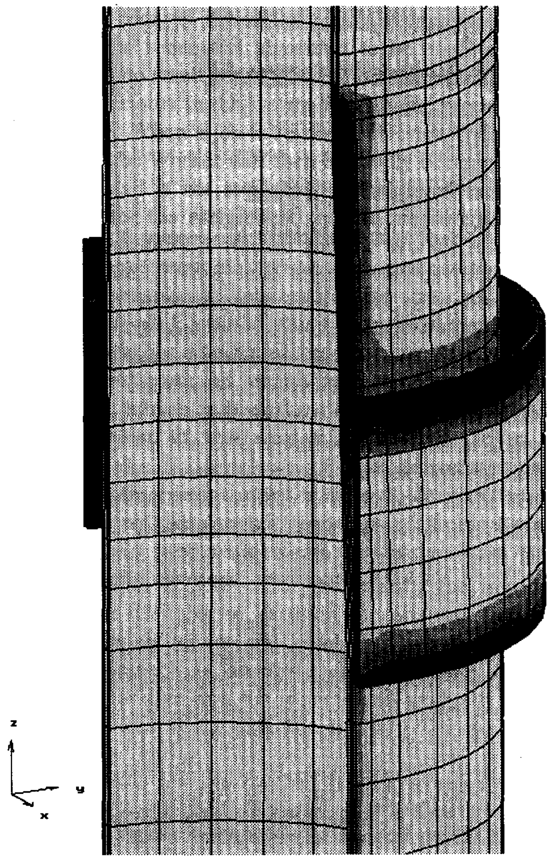

Fig. 3: Intensity of the current density.

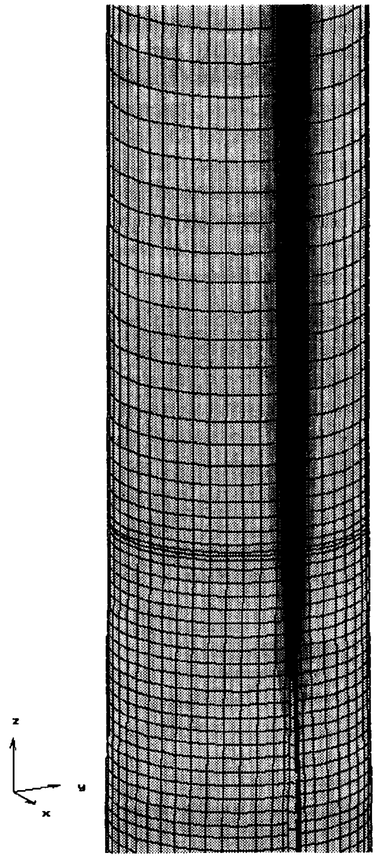

Fig. 4. Temperature distribution.

The maximum value of the current density is concentrated at the edges of the gap.

The most important criterion, however, is the stationary temperature distribution. At a feed velocity of 0.5 m/s, the test example achieved a temperature increase of 798.5 K at the welding point compared with temperature at the entrance of the tube. The maximum temperature is directly at the welding point (see Figure 4).

The calculation for the non-stationary temperature field is also carried out at the HP work station. The time required for making this calculation, a few hours, is comparatively shorter than the time required for the electromagnetic field.

V. Summary

The model shown here is very suitable for modelling the welding process for the longitudinal seam of a tube, since no crude simplifications were made. The problem is covered in its complete three-dimensional complexity. In addition, the calculation is possible in a broad spectrum of frequencies, right up to high frequencies. However, high frequencies require a finite element mesh with more nodes for the computation areas, so that computation technology capable of high efficiency will have to be employed. The installation of magnetic return elements (impeders) is just as possible as the taking into consideration of the energy of fusion in the calculation of the temperature field. The suitability of the model was proved by test calculations. It may now be employed for optimization calculations.

References

[1] W. Andree, "Ein Beitrag zur numerischen Berechnung induktiver Erwärmungsanordnungen mit Hilfe der Methode der finiten Elemente", Dissertation A, TH Ilmenau, 1982.

[2] U. Lüdtke, "Zur numerischen Berechnung dreidimensionaler elektromagnetischer Felder", Dissertation A, TH Ilmenau, 1990.

[3] K. Preis, "Anwendung der Methode der finiten Elemente zur numerischen Berechnung elektromagnetischer Felder", Habilitationsschrift, eingereicht an der TU-Graz, 1983.

[4] O. Biró, K. Preis, "On the use of the magnetic vector potential in the finite element analysis of three-dimensional eddy currents", *IEEE Transactions on Magnetics*, Vol. 25, NO. 4, July 1989, pp. 3145-3159.